Erik P. Schartner, Matthew R. Henderson, Malcolm Purdey, Deepak Dhatrak, Tanya M. Monro, P. Grantley Gill, and David F. Callen

Cancer detection in human tissue samples using a fiber-tip pH probe

Cancer Research, 2016; 76(23):6795-6801

Published version: http://dx.doi.org/10.1158/0008-5472.CAN-16-1285

Cancer detection in human tissue samples using a fibre-tip pH probe

Erik P. Schartner [1, a, b*], Matthew R. Henderson [1, a], Malcolm Purdey [a, b, c], Deepak Dhatrak [d], Tanya M. Monro [a, b, e], P. Grantley Gill [f], and David F. Callen [g]

[1] Joint first authors: these two authors contributed equally to this work

[a] Institute for Photonics and Advanced Sensing, School of Physical Sciences, The University of Adelaide, Adelaide, Australia

[b] ARC Centre for Nanoscale BioPhotonics, The University of Adelaide, Adelaide, Australia

[c] Heart Health Theme, South Australian Health and Medical Research Institute, Adelaide, Australia

[d] Department of Anatomical Pathology, Adelaide, Australia

[e] University of South Australia, Adelaide, Australia

[f] Department of Surgery, University of Adelaide & Breast, Endocrine & Surgical Oncology Unit, Royal Adelaide Hospital, Adelaide, Australia

[g] Centre for Personalised Cancer Medicine, School of Medicine, University of Adelaide, Adelaide, Australia

Running title: Cancer detection in human samples using a fibre-tip pH probe

Keywords: Breast cancer, melanoma/skin cancers, surgery:techniques and strategies, Prevention of second cancers, Optical sensing

Corresponding author: * erik.schartner@adelaide.edu.au

Funding Support: The authors acknowledge funding support from the National Breast Cancer Foundation Australia, an Australian Research Council linkage project LP110200736 and an ARC Georgina Sweet Laureate Fellowship.

Conflict of Interest: The authors declare no conflict of interest

Abstract

Intraoperative detection of tumorous tissue an important unresolved issue for cancer surgery. Difficulty in differentiating between tissue types commonly results in the requirement for additional surgeries to excise unremoved cancer tissue, or alternatively in the removal of excess amounts of healthy tissue. While pathological methods exist to determine tissue type during surgery, these methods can compromise post-operative pathology, have a lag of minutes to hours before the surgeon receives the results of the tissue analysis and are restricted to excised tissue. In this work we report the development of an optical fibre probe which could potentially find use as an aid for margin detection during surgery. A fluorophore doped polymer coating is deposited on the tip of an optical fibre, which can then be used to record the pH by monitoring the emission spectra from this dye. By measuring the tissue pH and comparing with the values from regular tissue the tissue type can be determined quickly and accurately. The use of a novel lift-and-measure technique allows for these measurements to be performed without influence from the inherent autofluorescence that commonly affects fluorescence-based measurements on biological samples. The probe developed here shows strong potential for use during surgery, as the probe design can be readily adapted to a low-cost portable configuration which could find use in the operating theatre. Use of this probe in surgery either on excised or in-vivo tissue has the potential to improve success rates for complete removal of cancers.

Introduction

Incomplete removal of malignant tumours continues to be a significant issue in cancer surgery. It increases the risk of local recurrence and impaired survival, and results in the need for additional surgery with associated attendant costs and morbidity (1-3). The excision of further benign tissue leads to poor cosmesis and impaired function, which assumes particular significance in some sites such as breast or head and neck cancer (1).

In the case of breast cancer, re-excision rates in excess of 20% have been widely reported, and this may lead to local recurrence (4-6). Standard pathology techniques such as the use of intraoperative cytology, selective margin re-excision based on specimen imaging and/or frozen section are time consuming, can potentially compromise post-operative pathological analysis, and show difficulty in accurate detection of small tumours (7-9). A recent trial reported higher rate of complete excision following systematic re-excision of the whole cavity at the time of partial mastectomy, compared with standard practice (5). Optical based imaging technologies have been shown to distinguish malignant from benign breast tissue in exploratory studies. These include methodology based on Raman spectroscopy (10,11), scanning in situ spectroscopy and mapping of whole specimens (12), combined diffuse reflectance spectroscopy and intrinsic autofluorescence (10,13), or multimodal optical imaging (14). These studies have been exploratory and have examined and mapped tissue distribution in whole excised specimens ex vivo. Potential limitations to their clinical use include the portability of equipment, tissue heterogeneity leading to scattering of light and autofluorescence and the time required to complete assessments.

The further development of rapid real-time techniques to detect small volumes of cancer at the margins of surgical specimens continues to be a priority in the treatment of cancer. Although breast cancer has been the principal focus of such investigation, the technology is also potentially important in other sites (15).

It has been shown in the literature that the extracellular pH in the vicinity of cancer is lowered, when compared to that of normal tissue in the same patient (16-19). While various methods exist to record tissue pH, to date it has been found to be difficult to accurately measure the pH of small areas of tissue

as would be required for the detection of cancer margins due primarily to the large size of conventional electrochemical surface pH probes which typically have a tip diameter in the order of 10mm.

Optical fibre based sensors have found extensive use in the areas of chemical (20-24), biological sensing (25-27), physical sensing for temperature (28-30), or structural health monitoring (31,32). Typically they are deployed in situations where measurements along the length of the fibre (distributed measurements) are required (33), however they also have strong potential for use in applications in difficult to reach locations. Fibre measurements can be performed at a position remote from the source and detection equipment. By creating a functional coating either along the length of the fibre, or on the end-face, the sensing region can be localised to the desired location depending on the application.

Here we report the first tissue pH measurements performed with an optical fibre tip pH probe on excised cancer samples. The optical fibre probe measures pH rapidly, in less than one minute, is simple to use, and does not leave a residue or stain that would affect later pathology testing. The probe consists of the pH sensitive fluorophore 5,6-carboxynapthofluorescein (CNF) (23), which changes colour with a change in the environmental pH. This fluorophore is embedded in an acrylamide polymer on the optical fibre tip, which is readout remotely via a laser at the other end of the fibre. Preliminary testing showed that this indicator displayed a good balance of an appropriate pH response range, broad optical spectra that could potentially be interrogated in the future with bulk optics, and good stability for repeat measurements over time. The fibre probe is flexible and robust, and has a small measurement area corresponding to the size of the 200 μm diameter optical fibre tip.

Measurements using organic fluorophores are commonly performed by monitoring the emission intensity of a single fluorescence band (wavelength), which is susceptible to errors arising from variations in the excitation light power, or photobleaching of the dye. The pH value is inferred by monitoring the ratio of two emission bands of the fluorophore. Ratiometric methods alleviate potential issues from photobleaching or coupling, allowing for measurements to be performed over a long period without the introduction of systematic errors.

A pervasive issue with optical based measurements of chemical or biological parameters is the presence of background autofluorescence from the tissue itself which is generated when the excitation light is incident on the tissue sample (34). While this can be reduced through the use of longer wavelength excitation sources, or pre-bleaching of the tissue, it remains a limitation in the majority of approaches to determine tissue measurements. This autofluorescence signal is difficult to remove through signal post-processing as it can vary significantly across a single sample (34). The novel architecture presented here can be utilised in a manner that avoids tissue autofluorescence impacting on the pH measurement. Here, the fibre-tip probe is placed in contact with the tissue surface and allowed to equilibrate, and is then lifted from the surface before the fluorophore is measured. This new “lift-and-measure” technique removes the interaction between the excitation source and the sample tissue. The fluorophore chemical structure is altered under different environmental pH conditions, which determines the varying emission properties. We propose that the sampling measurement induced structural change in the fluorophore is retained after lifting from the surface, and so the pH can be measured in the absence of autofluorescence. Calibration curve pH measurements were performed in a series of phosphate buffers, and these confirmed that a comparable response was seen between measurements with the probe dipped into the buffer and after lifting out from the buffer in air.

Using these techniques surgically excised human breast cancer and melanoma tissue samples were measured with the optical fibre pH probe at numerous locations over the sample surface, with the tissue type of each location confirmed later by histopathology.

Materials and Methods

Materials

Acrylamide (99%), N,N′-methylenebis(acrylamide) (99%), 3-(trimethoxysilyl)propyl methacrylate (98%), triethylamine (99%), monobasic and dibasic potassium hydrogen phosphate were obtained from Sigma-Aldrich Chemical Co. (St. Louis, MO). CNF was obtained from Santa Cruz Biotechnology, (Dallas, TX). Potassium phosphate buffers were made up from appropriate ratios of

monobasic and dibasic potassium hydrogen phosphate to an ionic strength of 0.1 mM, covering a pH range from 6.0 to 8.8.

The polymer solution consisted of (by weight) 27% acrylamide, 3% bis-acrylamide and 70% pH 6.5 potassium phosphate buffer, with 0.4 mg/mL CNF and 40 µL/mL triethylamine. The solution was ultrasonicated until all solid components were fully dissolved and used immediately.

Fibre probe

The optical setup was configured as shown in Figure 1. Acrylamide was attached to the fibre tip by photopolymerisation using a 405 nm laser for two seconds at a coupled power of 13 mW. The CNF fluorophore was excited with a blue 473 nm laser for the pH measurements. The two lasers were aligned to be collinear into the microscope objective, such that no realignment was required between the coating step and subsequent measurements. Silica multi-mode fibre was used for all coating trials (Thorlabs UG200UEA or Ocean Optics 200 µM UV/VIS).

The fibre was cleaved to expose a fresh surface for polymer attachment. The fibre tip was dipped into a 2% solution of 3-(trimethoxysilyl)propyl methacrylate in pH 3.5 HCl for one hour, after which the fibre was removed and dried with nitrogen. A 405 nm laser source (Crystalaser 25 mW) was coupled into the input end of the optical fibre, and the power optimised with a calibrated photodiode. Fibre tips were then dipped into the acrylamide polymer solution described above, and illuminated with the 405 nm source for two seconds with a coupled laser power of 15±0.2 mW to photopolymerise the acrylamide polymer onto the fibre tip.

pH measurement

A schematic of the optical setup is shown in Figure 1. A 473 nm laser (Toptica iBeam Smart) was used to excite the CNF fluorophore. The resulting emission of the CNF consists of two peaks, at approximately 565 nm and 705 nm, with an intensity ratio dependent on the pH of the environment around the fluorophore.

To excite the CNF fluorophore, the 473 nm laser was coupled into the distal end of the probe fibre. The coupled laser light then excites the fluorophore-doped probe tip, and a portion of this fluorescent light is then captured into a back-propagating mode in the fibre. The fluorescent signal then passes through a 473 nm long-pass filter (Semrock EdgeBasic) to remove excess excitation light, before being coupled into a spectrometer (Horiba iHR320) via a 200 µm optical fibre patch cable.

Since the surface pH of tissue biopsies deteriorated slowly when exposed to the atmosphere, before measuring with the probe fresh surfaces were exposed by excision.

Spectral analysis & Lift-and-measure measurement technique

The ratio of the two CNF fluorophore emission peaks was used to measure the pH response of the probe. Spectra were post-processed by integrating the signal under the two peaks, from 500-635 nm and from 635-900 nm, and dividing the area of the first peak by the area of the second peak giving the fluorescence ratio for that particular probe location.

Samples were first measured with the probe tip in contact with the sample. The probe was then lifted from the surface, and the measurement repeated. Removal of the probe tip from the sample eliminates autofluorescence from the tissue sample, such that the only contribution to the observed signal is from the fibre sensor itself.

Probe verification

The pH response of the optical fibre probe was verified by dipping into a series of 0.1 mM potassium phosphate buffer solutions. Measurements were performed both in the solution and in air after removing from the buffer, to simulate the lift-and-measure technique described above and as used for the human tissue samples.

Autofluorescence measurements

Sheep tissue samples were spiked with 1 M hydrochloric acid (Sigma-Aldrich) or 1M sodium hydroxide (Sigma-Aldrich) to obtain acidic or basic samples respectively. Measurements were

performed using the lift-and-measure technique described above, in an identical fashion to that used for the human tissue samples.

Tissue samples

The project was approved by the Royal Adelaide Hospital Research Ethics Committee and patients gave individual informed consent for their participation.

Research specimens obtained at surgery were placed on ice and transported to the pathology laboratory where they were inked and sliced for normal diagnostic processing. Four mastectomy specimens, one axillary clearance for recurrent breast cancer and three cases of metastatic melanoma were included (Table 1). Fresh tissue not required for diagnostic evaluation was utilised for the pH evaluation experiments within one hour of excision at surgery.

Pathology verification

The location of each pH measurement using the optical fibre probe were photographically recorded to enable correlation with presence of non-malignant or cancer tissue as determined by subsequent histopathology.

Following the pH measurements, the tissue was fixed in 10% buffered formalin for 24 hours and photographed. The presence of cancer or normal tissue at the measurement sites was then histologically assessed in Haematoxylin and eosin (H&E) stained paraffin embedded sections. The occurrence of either cancer or normal tissue at each measurement site was determined by using both the macroscopic photographs and the H&E stained sections for accuracy. The H&E sections were also used for tumour typing, and determination of non-malignant tissue as fat or fibrosis. Correlation was then made with the site of probe and the type of underlying tissue from which the pH reading was taken. For the majority of the cases there was a single localised tumour but several cases had multifocal tumours in the specimen (Table 1).

Results

Effect of tissue autofluorescence

A background tissue autofluorescence signal is generated when the probe excitation light is incident on the tissue sample. The autofluorescence spectrum can vary significantly across the sample and so is difficult to remove with data post-processing techniques, such as subtraction. An example of tissue autofluorescence is shown in Figure 2, where spectra have been recorded with the probe both touching and lifted from the tissue surface, for sheep tissue samples spiked with hydrochloric acid (acidic) or sodium hydroxide (basic) solutions.

As shown in Figure 2, the autofluorescence background can form a significant fraction of the total signal strength and can form a significant contribution to the apparent measured ratio. The tissue samples were spiked with acidic and basic solutions to show that the autofluorescence background affects measurements in both high and low pH environments

Probe response to pH and verification of lift-and-measure technique

To reduce the impact of autofluorescence on the pH measurements a novel “lift-and-measure” technique was devised. The probe response to pH was first recorded with a series of PBS buffer solutions, measuring the response both before and after removal from the solution (Figure 3).

From these results it can be seen that the probe has a similar response to pH both in solution and after removal, with a small shift in the pH response curve between the two, and so it can be concluded that the lift-and-measure pH measurement is a valid reading of the surface tissue pH. Upon removal of the fibre from the solution changes in the fluorescence spectra were observed for one - five seconds, which is interpreted as the evaporation of the solvent from the tip of the fibre. After this rapid change the signal was observed to be stable for a period of at least ten minutes. Preliminary experiments demonstrated that the pH shift of this fluorophore was extremely well suited to differentiation between healthy and tumorous tissue, with large shifts observed in the fluorescence ratio between the two tissue types.

Figure 3a shows the fluorescence response of the CNF with varied pH. As the buffer pH increases, the first peak decreases in intensity while the second peak increases. Integration of the two fluorescence bands to obtain the fluorescence ratio gives the results shown in Figure 3b. This ratiometric behaviour allows for the pH to be interpreted with little dependence on the excitation power or fluorophore density. If the excitation intensity is increased the two bands will increase proportionally, removing the intensity dependence which typically restricts the precision of intensity-based fluorophore measurements. This property also minimises variations in pH signal response between probes, simplifying fabrication requirements.

The structure of CNF both before and after reaction with hydrogen ions is shown in Figure 4. As the probe equilibrates with the pH of the solution, each CNF molecule will be in either the protonated acid form or in the deprotonated form that favours formation of the lactone. We postulate that because each CNF molecule is locked in protonated or deprotonated form, the fluorescence emission profile of the probe will reflect the equilibrium achieved in solution. The subsequent result of this is that the probe retains a "memory" of the pH of the solution into which it was last immersed. This particular property of the fluorophore allows for the use of the lift-and-measure technique, with measurements to be performed after the removal of the probe from the surface of the tissue sample to reduce the observed tissue autofluorescence.

Tissue measurements

Tissue surface measurements were obtained from four melanoma and four breast cancer samples. Figure 5a shows the individual measurement results, with tissue type determined after each experiment by pathology tests. Data was normalised to the mean value of the normal tissue results to simplify comparison between samples, the results of which are shown in Figure 5a. The mean and standard deviation values for the individual samples are shown in Table 1, along with descriptions of the specimen and tumour type for each of the measured samples. The receiver operating characteristic (ROC) curve for the normalised data is shown in Figure 5b.

An example of a measured sample is shown in Figure 6 below. This photograph taken before optical measurements was performed has the probe sampling locations marked for Sample 2 (Metastatic melanoma in multiple lymph nodes). The tissue type in each of these locations was determined using pathological analysis methods described earlier.

From the results shown in Figure 5a it can be seen that typically the tumour samples are significantly more acidic than normal tissue samples. Applying the Mann Whitney U test on the dataset showed significant differences between healthy and tumorous tissue, with $p<0.001$. Utilising the ROC curve in Figure 5b a threshold for these preliminary values was defined, with a pH ratio of 1.35 showing a sensitivity of 88%, and a selectivity of 90%.

As can be seen from the data in Table 1, some variation in values is observed between samples for the tumour tissue samples, with the majority of samples however still showing a statistically significant difference in tissue pH between the tumour and normal tissue samples.

Necrotic tumour and fibrosis tissue types were also measured during trials, with results suggesting that the probe is also able to discriminate effectively between these tissue types as well. Necrotic tumour samples were observed to display a similar pH to regular cancer samples, while fibrosis samples showed a similar pH to normal tissue.

Discussion

These results show that cancerous tissue can be effectively differentiated from normal tissue in fresh human tissue biopsies by measurement of the tissue pH. The use of an optical probe allows for measurements to be performed rapidly with high spatial resolution. Currently our results show that measurements can be performed using an optical probe with a diameter of 200 μm, equivalent to an area in the order of five to ten cells wide, with the potential to reduce this to the measurement of single cells by reducing the size of the fibre probe by tapering the fibre tip (25). The use of the lift-and-measure technique allows measurements to be performed without the influence of the tissue autofluorescence that typically restricts the performance of optical sensors. Minimal effects from

photobleaching were observed, with the sensor showing high levels of stability even with repeat scans during tissue measurements.

The performance of the pH probe in this preliminary study was comparable or exceeded that described by a commercially available product, the Marginprobe (88% sensitivity at 1.35 threshold marked in Figure 5a, versus 84-68%) by Pappo et al. (35,36). The variations observed a subset of the tissue samples may have been due to probe function, or alternatively failure to accurately collocate the tissue measurement and the final pathology samples. Measures to address this latter possibility have been included in current studies. Heterogeneity of tissue elements can vary widely within tumours and normal breast tissue. This was shown to contribute to a variation in sensitivity in the detailed initial evaluation of the Marginprobe by Pappo (35). Similar criticisms have been made with respect to the range of other optical methods (37). A similar consideration could have contributed to the variation we observed with low values for two tumours.

Additional improvements to the optical probe, such as the use of multi-core imaging fibre could also result in an increase in sample throughput, by measuring the tissue pH over a larger area with improved spatial resolution compared to the multi-mode fibre which was utilised here, which gives a single discrete pH measurement at each sampling location.

This is an important step towards the development of a real-time sensor which can be used *in vivo* at the time of surgery to determine the presence of cancer at surgical margins. The rapid response of the optical probe gives an indication of the tissue type in real-time. Measurement time could potentially be controlled by varying the thickness of the polymer layer, as testing showed a thinner layer gives faster response however at the cost of reduced signal intensity. The use of such a fibre sensor to give an immediate indication of tissue type has the potential to reduce the need for repeat surgery by increasing the success rate of complete cancer removal. It offers the potential for greater precision and smaller excision volumes during surgery compared with a complete cavity shave, (5) and a small footprint compared with other techniques. The low level of complexity involved in determining tissue type using the probe also gives rise to the potential for the use of this probe in a portable configuration. Given its

construction is based on optical fibres it also has the potential for wider use in other sites and more deeply situated tumours as allowed by endoscopic or image-guided devices.

Acknowledgements

The authors would like to thank Prof. Mark Hutchinson for assistance with statistical analysis, Dr Georgios Tsiminis for useful discussions, and Mr Sebastian Ng and Ms. Catherine Lang for assistance with some of the experiments.

References

1. Cabioglu N, Hunt KK, Sahin AA, Kuerer HM, Babiera GV, Singletary SE, et al. Role for intraoperative margin assessment in patients undergoing breast-conserving surgery. Annals of Surgical Oncology 2007;14(4):1458-71.
2. Rouzier R, Extra J-M, Carton M, Falcou M-C, Vincent-Salomon A, Fourquet A, et al. Primary chemotherapy for operable breast cancer: incidence and prognostic significance of ipsilateral breast tumor recurrence after breast-conserving surgery. Journal of clinical oncology 2001;19(18):3828-35.
3. Elkhuizen PH, van de Vijver MJ, Hermans J, Zonderland HM, van de Velde CJ, Leer J-WH. Local recurrence after breast-conserving therapy for invasive breast cancer: high incidence in young patients and association with poor survival. International Journal of Radiation Oncology* Biology* Physics 1998;40(4):859-67.
4. Jeevan R, Cromwell D, Trivella M, Lawrence G, Kearins O, Pereira J, et al. Reoperation rates after breast conserving surgery for breast cancer among women in England: retrospective study of hospital episode statistics. 2012.
5. Chagpar AB, Killelea BK, Tsangaris TN, Butler M, Stavris K, Li F, et al. A randomized, controlled trial of cavity shave margins in breast cancer. New England Journal of Medicine 2015;373(6):503-10.

6. McCahill LE, Single RM, Bowles EJA, Feigelson HS, James TA, Barney T, et al. Variability in reexcision following breast conservation surgery. Jama 2012;307(5):467-75.
7. Pleijhuis RG, Graafland M, de Vries J, Bart J, de Jong JS, van Dam GM. Obtaining adequate surgical margins in breast-conserving therapy for patients with early-stage breast cancer: current modalities and future directions. Annals of surgical oncology 2009;16(10):2717-30.
8. Singletary SE. Surgical margins in patients with early-stage breast cancer treated with breast conservation therapy. The American journal of surgery 2002;184(5):383-93.
9. Unzeitig A, Kobbermann A, Xie X-J, Yan J, Euhus D, Peng Y, et al. Influence of surgical technique on mastectomy and reexcision rates in breast-conserving therapy for cancer. International journal of surgical oncology 2012;2012.
10. Keller MD, Vargis E, de Matos Granja N, Wilson RH, Mycek M-A, Kelley MC, et al. Development of a spatially offset Raman spectroscopy probe for breast tumor surgical margin evaluation. Journal of biomedical optics 2011;16(7):077006-06-8.
11. Haka AS, Volynskaya Z, Gardecki JA, Nazemi J, Lyons J, Hicks D, et al. In vivo margin assessment during partial mastectomy breast surgery using Raman spectroscopy. Cancer Research 2006;66(6):3317-22.
12. Krishnaswamy V, Laughney AM, Wells WA, Paulsen KD, Pogue BW. Scanning in situ spectroscopy platform for imaging surgical breast tissue specimens. Optics express 2013;21(2):2185-94.
13. Lue N, Kang JW, Yu C-C, Barman I, Dingari NC, Feld MS, et al. Portable optical fiber probe-based spectroscopic scanner for rapid cancer diagnosis: a new tool for intraoperative margin assessment. PLoS One 2012;7(1):e30887.
14. Patel R, Khan A, Wirth D, Kamionek M, Kandil D, Quinlan R, et al. Multimodal optical imaging for detecting breast cancer. Journal of biomedical optics 2012;17(6):0660081-89.
15. Poh CF, Zhang L, Anderson DW, Durham JS, Williams PM, Priddy RW, et al. Fluorescence visualization detection of field alterations in tumor margins of oral cancer patients. Clinical Cancer Research 2006;12(22):6716-22.

16. Gerweck LE. Tumor pH: implications for treatment and novel drug design. 1998. Elsevier. p 176-82.
17. Gerweck LE, Seetharaman K. Cellular pH gradient in tumor versus normal tissue: potential exploitation for the treatment of cancer. Cancer research 1996;56(6):1194-98.
18. Stubbs M, McSheehy PM, Griffiths JR, Bashford CL. Causes and consequences of tumour acidity and implications for treatment. Molecular medicine today 2000;6(1):15-19.
19. Švastová E, Hulíková A, Rafajová M, Zat'ovičová M, Gibadulinová A, Casini A, et al. Hypoxia activates the capacity of tumor-associated carbonic anhydrase IX to acidify extracellular pH. FEBS letters 2004;577(3):439-45.
20. Wolfbeis OS. Fiber-optic chemical sensors and biosensors. Analytical Chemistry 2008;80(12):4269-83.
21. Warren-Smith SC, Heng S, Ebendorff-Heidepriem H, Abell AD, Monro TM. Fluorescence-based aluminum ion sensing using a surface-functionalized microstructured optical fiber. Langmuir 2011;27(9):5680-85.
22. Peterson JI, Goldstein SR, Fitzgerald RV, Buckhold DK. Fiber optic pH probe for physiological use. Analytical Chemistry 1980;52(6):864-69.
23. Song A, Parus S, Kopelman R. High-performance fiber-optic pH microsensors for practical physiological measurements using a dual-emission sensitive dye. Analytical chemistry 1997;69(5):863-67.
24. Schartner EP, Tsiminis G, François A, Kostecki R, Warren-Smith SC, Nguyen LV, et al. Taming the Light in Microstructured Optical Fibers for Sensing. Int J Appl Glass Sci 2015;6(3):229-39.
25. Tan W, Shi Z-Y, Smith S, Birnbaum D, Kopelman R. Submicrometer intracellular chemical optical fiber sensors. Science 1992;258(5083):778-81.
26. Shortreed M, Kopelman R, Kuhn M, Hoyland B. Fluorescent fiber-optic calcium sensor for physiological measurements. Analytical chemistry 1996;68(8):1414-18.

27. Warren-Smith SC, Nie G, Schartner EP, Salamonsen LA, Monro TM. Enzyme activity assays within microstructured optical fibers enabled by automated alignment. Biomedical optics express 2012;3(12):3304-13.

28. Hocker G. Fiber-optic sensing of pressure and temperature. Applied optics 1979;18(9):1445-48.

29. Kurashima T, Horiguchi T, Tateda M. Distributed-temperature sensing using stimulated Brillouin scattering in optical silica fibers. Optics Letters 1990;15(18):1038-40.

30. Schartner EP, Monro TM. Fibre Tip Sensors for Localised Temperature Sensing Based on Rare Earth-Doped Glass Coatings. Sensors 2014;14(11):21693-701.

31. Tennyson R, Mufti A, Rizkalla S, Tadros G, Benmokrane B. Structural health monitoring of innovative bridges in Canada with fiber optic sensors. Smart materials and Structures 2001;10(3):560.

32. Majumder M, Gangopadhyay TK, Chakraborty AK, Dasgupta K, Bhattacharya DK. Fibre Bragg gratings in structural health monitoring—Present status and applications. Sensors and Actuators A: Physical 2008;147(1):150-64.

33. Bao X, Webb DJ, Jackson DA. 32-km distributed temperature sensor based on Brillouin loss in an optical fiber. Optics Letters 1993;18(18):1561-63.

34. Neumann M, Gabel D. Simple method for reduction of autofluorescence in fluorescence microscopy. Journal of Histochemistry & Cytochemistry 2002;50(3):437-39.

35. Pappo I, Spector R, Schindel A, Morgenstern S, Sandbank J, Leider LT, et al. Diagnostic performance of a novel device for real-time margin assessment in lumpectomy specimens. Journal of Surgical Research 2010;160(2):277-81.

36. Allweis TM, Kaufman Z, Lelcuk S, Pappo I, Karni T, Schneebaum S, et al. A prospective, randomized, controlled, multicenter study of a real-time, intraoperative probe for positive margin detection in breast-conserving surgery. The American Journal of Surgery 2008;196(4):483-89.

37. Thill M, Röder K, Diedrich K, Dittmer C. Intraoperative assessment of surgical margins during breast conserving surgery of ductal carcinoma in situ by use of radiofrequency spectroscopy. The Breast 2011;20(6):579-80.

Tables

Sample	Specimen	Tumour type	Number of measurements	Tumour mean and std. dev.	Normal mean and std. dev.
1	Left inguinal lymph node dissection	Metastatic melanoma	12	5.3 ± 1.3	1.0 ± 0.1
2	Left axillary clearance	Metastatic melanoma in multiple lymph nodes	11	3.4 ± 1.0	1.0 ± 0.07
3	Skin excision, right groin	Subcutaneous deposit of metastatic melanoma	15	1.7 ± 0.4	1.0 ± 0.5
4	Left mastectomy	Grade II infiltrating ductal carcinoma	12	1.31 ± 0.31	1.0 ± 0.2
5	Left mastectomy	Grade II infiltrating ductal carcinoma	11	2.7 ± 1.5	1.0 ± 0.8
6	Right mastectomy	Invasive metaplastic carcinoma (spindle cell carcinoma with anaplasia)	20	3.3 ± 0.8	1.0 ± 0.4
7	Left mastectomy	Grade III infiltrating ductal carcinoma	11	6.9 ± 2.6	1.0 ± 0.04
8	Left axillary clearance	Multiple tumour deposits of infiltrating ductal carcinoma ranging 4 mm to 20 mm	12	1.9 ± 0.3	1.0 ± 0.1

Table 1 - Summary of measurements

Figure Legends

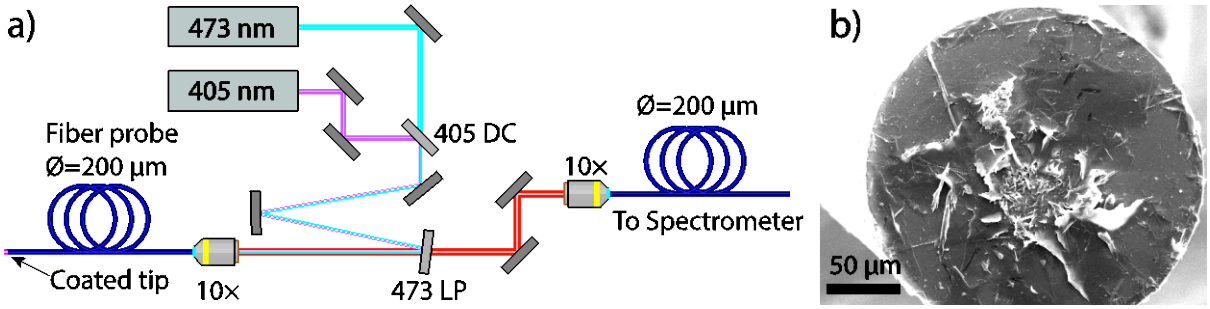

Figure 1 – Experimental details for measurements (a) Schematic for coating and pH measurement trials. (b) Scanning electron microscope image showing an example of the polymer coatings obtained.

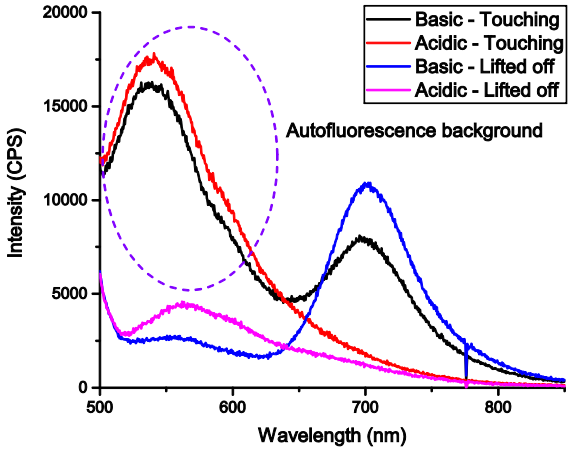

Figure 2 - Spectra of fibre pH probe measuring the surface of tissue spiked with an acidic or basic solution. Measurements were performed both touching the tissue surface and in air using the lift-and-measure technique.

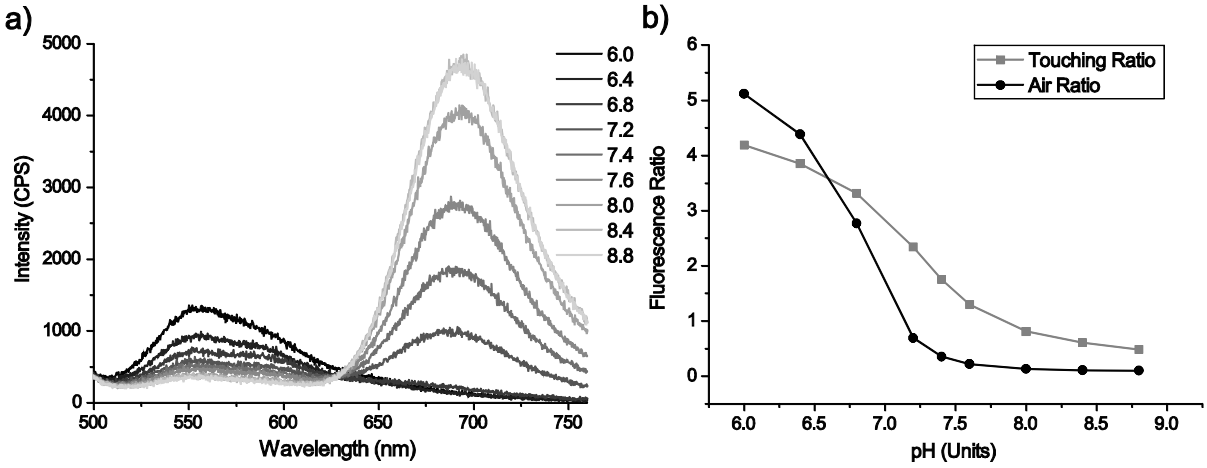

Figure 3. Characterization of the polymer functionalized probe (a) Emission spectra of the CNF fluorophore at different environmental pH values showing the ratiometric response. Spectra taken in air after 20s immersion in buffer. (b) Calibration curve for the fibre pH probe both dipped into a buffer (Touching, grey squares) and in air after dipping (Air, black circles).

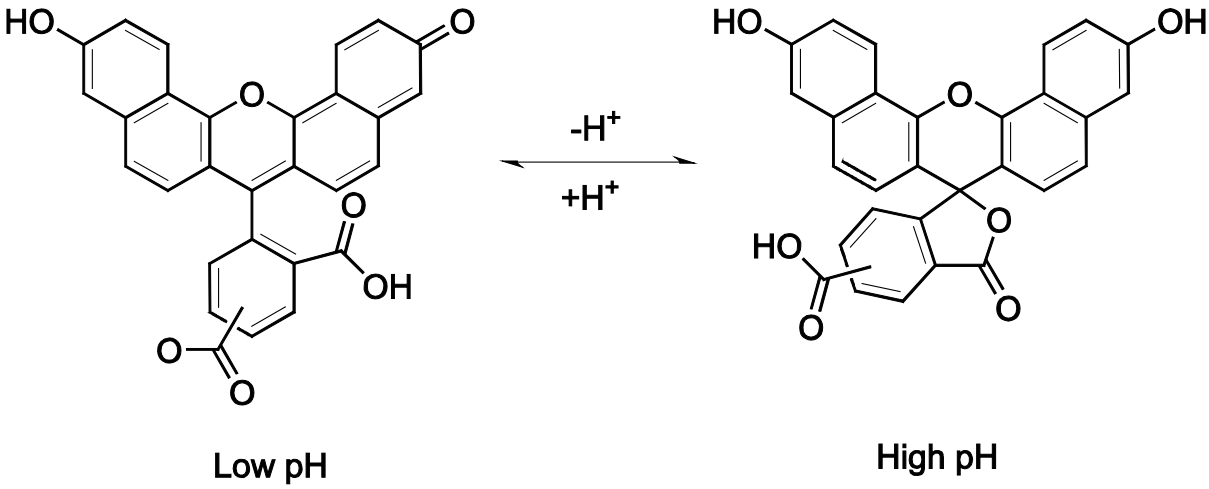

Figure 4. Chemical structure of CNF, illustrating the structural change that occurs due to pH.

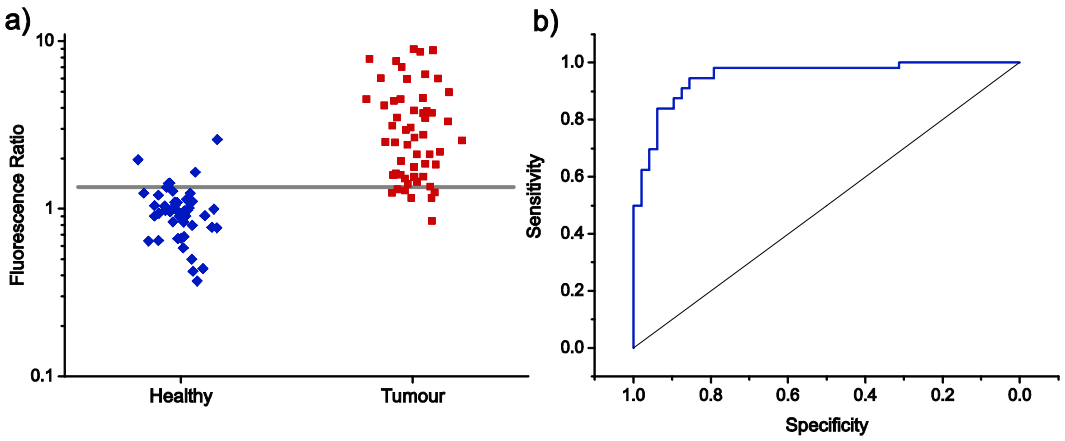

Figure 5. Results obtained from use of the optical fiber pH probe on excised human tissue samples (a) Scatter plot showing the measured fluorescence ratio using the optical fibre tip pH probe, obtained from normal (fat and breast tissue) and tumour surface tissue measurements across eight tissue samples. Probe measurement locations were subsequently pathology tested to confirm tissue type. For each sample, the data was normalised to the mean value of the corresponding normal tissue dataset, with the mean and standard deviation for each individual sample shown in Table 1. Tumour (grey) and normal (black) measurement datasets are shown, with the experimentally derived threshold value used to determine the accuracy and specificity of the optical measurement technique marked in grey (b) Receiver operating characteristic (ROC) curve for data shown in Figure 5a

Figure 6. Example photograph of Sample 2 (Metastatic melanoma in multiple lymph nodes), with probe sampling locations marked on the image.